Velocity versus temperature relation for solidification and melting of silicon: A molecular-dynamics study

Mark D. Kluge* and John R. Ray
Kinard Laboratory of Physics, Clemson University, Clemson, South Carolina 29634-1911
(Received 20 July 1988)

We report on molecular-dynamics simulations to determine the steady-state velocity versus temperature relation for (001) solidification and melting of silicon using the Stillinger-Weber potential to model the interactions between the silicon atoms. Down to 250 K of undercooling, the simulation values show good agreement with experimental results. The slope of the temperature velocity relation near the melting point is reported as $(-15\pm5$ K)/(m/s) whereas we find the slope of the transition-state curve that we fitted to the simulation values has a slope $(-9.8$ K)/(m/s) at the melting point. However, since Stillinger-Weber amorphous silicon is not formed easily by cooling the melt our simulations do not show the growth into amorphous silicon at the critical velocity of ≈ 15 m/s (undercooling below ≈ 250 K) that is observed experimentally. Instead in our simulations the velocity of growth into crystalline silicon increases to a maximum of 19.4 m/s at 1350 K and then decreases to at least 1050 K. At 1000 K, the system grows a few incomplete planes, which we suggest may be associated with the growth of amorphous silicon. At 950 K, we did not detect any growth during the 115 ps of the simulation. We also did not observe growth at 1600 or 1700 K over the 115 ps of these simulations. The simulation velocity versus temperature relation shows asymmetry in the solidification and melting portions of the curve with no discontinuity in slope at the melting point. We fitted our simulation velocity versus temperature relation by using the transition-state theory parametrized to Stillinger-Weber silicon. The transition-state theory gives a good qualitative description of the simulation values at all temperatures. It is interesting that the transition-state theory also fits the experimental values for crystallization even though it is parametrized for Stillinger-Weber silicon. The results of these epitaxial-growth studies of silicon are important for studies attempting to model the growth of layered structures by atom deposition with use of molecular dynamics with the Stillinger-Weber potential. Our results show that, even if the deposited atoms have kinetic energies 60% below the melting temperature, the growth of the crystal may be caused by liquid epitaxial growth with one (001) plane grown every 10 ps.

I. INTRODUCTION

Most solidification and melting processes involve the motion of a liquid-solid interface, that is, they are heterogeneous. Using electrical conductance techniques, the motion and velocity of the liquid-solid interface, in silicon, can now be measured directly.[1-9] Theoretical discussions of these solidification and melting processes have mainly been associated with various modifications in the transition-state theory of crystal growth.[10,11]

In the present paper[12] we report on molecular-dynamics calculations in which we have determined the steady-state interface velocity in solidification and melting as a function of temperature, undercooling or overheating for the Stillinger-Weber model of silicon.[13] Although the Stillinger-Weber model of silicon is known to have its shortcomings it does give reasonable agreement for many properties of silicon, including the melting temperature and the liquid structure factor.

As an example of the quality of the agreement with observed properties that is obtained using the Stillinger-Weber potential to model the silicon interaction we mention a recent paper[14] which shows that the softening in the elastic properties between crystalline and amorphous silicon is quite accurately described using this model potential. This latter paper also contains references to several other studies of silicon using the Stillinger-Weber potential.

One of the main problems with the Stillinger-Weber potential is that it does not lead *directly* to the formation of amorphous silicon upon rapid cooling of the liquid, whereas experiments show that amorphous silicon is easily formed in this way. The fact that the Stillinger-Weber potential does not easily form amorphous silicon, upon cooling the liquid, was first shown by Broughton and Abraham.[15] We were able to produce a model of amorphous silicon[16,17] by rapidly cooling the liquid and then expanding the supercooled system. This procedure does produce a model of amorphous silicon with several correct properties,[14,16,17] but one has interfered with the kinetics in an ad hoc manner; the amorphous system is not formed by simply cooling the liquid as is found experimentally. As we shall see the difficulty of forming amorphous silicon with the Stillinger-Weber potential also leads to disagreements between the epitaxial growth simulations reported on in this paper and experimental findings.

It should also be mentioned that what is formed when liquid Stillinger-Weber silicon is rapidly cooled (10^{13} K/s) is a supercooled liquid which is called the intermediate state in Ref. 17. This intermediate state is metastable over long times on a molecular-dynamics scale, hundreds

of ps. This long-lived metastable state is not observed experimentally, although it is not clear that present experimental results rule out such a metastable state on the time scales under discussion in the simulations.

In Sec. II we briefly discuss the Stillinger-Weber potential and in Sec. III we give the details of the simulations that are used to determine the steady-state solidification and melting velocities. In Sec. IV we describe the method of obtaining these velocities from our simulations. In Sec. V we discuss the results for all temperatures studied along with a comparison to related theoretical and experimental results. Finally in Sec. VI we present a summary and our conclusions.

II. STILLINGER-WEBER POTENTIAL

In a substance where the atoms interact through strong directional bonds, as in the tetrahedral semiconductors, it is necessary to include at least two- and three-body interactions. The two- and three-body interactions arrived at by the Stillinger and Weber[13] have the form

$$U_2(r_{ab}) = A\,(Br_{ab}^{-p} - r_{ab}^{-q}) h_\beta(r_{ab}) \,, \tag{2.1}$$

$$U_3(r_{ab}, r_{ac}, r_{bc}) = h_{cab} + h_{abc} + h_{bca} \,, \tag{2.2}$$

$$h_{cab} = \lambda h_\gamma(r_{ab}) h_\gamma(r_{ac}) (\cos\theta_{cab} + \tfrac{1}{3})^2 \,, \tag{2.3}$$

where r_{ab} is the distance between atoms a and b, $h_\delta(r) = \exp[\delta(r-a)^{-1}]$ for $r < a$ and vanishes for $r > a$; θ_{cab} is the angle between the vector r_{ab} and r_{ac}. In these equations r is expressed in units where unit distance corresponds to $\sigma = 2.0951$ Å, the energy is expressed in units where the unit of energy is $\epsilon = 3.4723 \times 10^{-12}$ erg. Stillinger and Weber indicated that they carried out a limited search over the parameters in Eqs. (2.1)–(2.3) to obtain the values $A = 7.049\,556$, $B = 0.602\,225$, $p = 4$, $q = 0$, $\beta = 1$, $a = 1.8$, $\lambda = 21$, and $\gamma = 1.2$. The unit of time is chosen as $\sigma(m/\epsilon)^{1/2} = 7.66 \times 10^{-14}$ s, where m is the mass of the silicon atom $m = 46.62 \times 10^{-24}$ g. The smooth cut-off distance a in U_2 and U_3 is slightly less than the second-neighbor distance in the 0 K crystal. At this distance the potentials along with all their derivatives go to zero continuously.

Note that the three-body energy Eq. (2.2) vanishes for the perfect tetrahedral angle $\cos\theta = -\frac{1}{3}$ and, therefore, also for the static diamond lattice. An important part of the parameter search carried out by Stillinger and Weber was to ensure that the diamond lattice have the lowest energy compared to several other simple lattices *sc*, *bcc*, *fcc*, ... The three-body energy effectively destabilizes these other lattices. Also the crystal melts at approximately the observed temperature, 1683 K at zero pressure.

III. DETAILS OF SIMULATIONS

Our simulations started from a well-equilibrated solid of 432 particles interacting via the Stillinger-Weber potential at a temperature of 1450 K. The solidification and melting simulations were all associated with liquid epitaxial crystallization or melting along the [001] direction. The [001] direction in our sample of 432 particles is along the z axis. There are 24 (001) planes in this sample each containing 18 particles. The left-hand side of the sample is located near $z = 0$, while the right-hand side is located near $z = 33$ Å. The positions of the particles in the two left most planes (planes 1 and 2) are always held fixed while the next two planes (planes 3 and 4) are used to add and subtract energy necessary to keep the temperature (average kinetic energy of all the particles except those in the first two planes) of the sample approximately constant during the solidification or melting process. During crystal growth energy must be extracted in order to keep the temperature of the sample constant. While in melting, energy must be added; these energies are associated with the latent heat of the first-order phase transformation under study. The solidification or melting processes takes place in planes 12–24 which are far enough removed from planes 3 and 4 so that the energy extraction or addition has a small disturbance on the dynamics of the solidification or melting processes. Periodic boundary conditions are imposed on the sample in the directions transverse to the z axis, while the boundary condition in the z direction, on the right-hand side of the sample, is a free boundary. All simulations were carried out with fixed area in the x-y planes. The iteration time step was 7.66×10^{-16} s.

In order to start the growth experiments we held the positions of particles in planes 3–12 fixed and increased the energy of the particles in planes 13–24 in order to melt this portion of the sample. After melting the right-hand side of the sample, planes 13–24, the system was run at a high temperature 2300 K for a long period of time, 50×10^3 time steps. This well-equilibrated liquid was then cooled to 1450 K and equilibrated as a supercooled liquid at this temperature. Next the particles in planes 3–12 were allowed to participate in the dynamics by giving them the freedom of moving. After allowing the particles in planes 3–12 to participate in the dynamics, we ran the system for 20×10^3 time steps and then began collecting data. The system in this configuration consists of a hot solid in contact with a supercooled liquid at a temperature near 1450 K and time zero is measured from this configuration.

From time zero the system was allowed to evolve for 150×10^3 time steps or 115 ps with particle configurations saved after each 10×10^3 time steps for analysis of the growth process. Every 20 time steps energy is either added or subtracted by scaling the velocities of particles in planes 3 and 4 in order to keep the temperature of the system near the desired value which is 1450 K for the run under discussion. By this procedure the temperature of the system is held to within a few degrees of the desired temperature over the entire simulation of 150×10^3 time steps. The heat released by the solidification equals the heat flow into the solid and the velocity of crystallization is associated with thermal transport away from the crystallization region.

In Fig. 1 we show the density profile, in arbitrary units, at 20×10^3 time steps into the simulation. By this time there is one almost fully grown plane, plane 13, and one partially grown, plane 14. In this figure the two left most planes are planes 1 and 2 whose particles are held con-

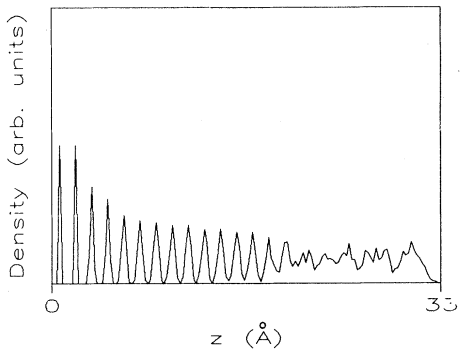

FIG. 1. Density profile, in arbitrary units, at time step 20×10^3 into the 1450 K solidification simulation. The particles in the two left most planes are held fixed. The simulation starts by melting the right half of the sample and then lowering its temperature to 1450 K and then allowing the system, which consists of a solid at 1450 K in contact with a liquid at 1450 K to evolve while maintaining the temperature of the system constant.

stant in the simulations. In Figs. 2–5 we show the density profile of the system at 50×10^3, 80×10^3, 110×10^3, and 140×10^3 time steps into the simulation. These figures clearly show the continual growth of crystalline planes during the simulation. Note that in these figures the growth appears monotonic in time, however, on shorter time scales the growth process is quite involved and not monotonic; that is, planes partially grow and then disorganize on a short time scale but on a longer time scale there is net growth of the crystalline portion of the sample. As the crystal grows the latent heat of transformation which is released is conducted through the sample and extracted at planes 3 and 4. Without this temperature control the temperature of the system would increase during the growth process, and we would not have isothermal growth and would, therefore, not be able to determine the steady-state growth velocity as a function of the temperature.

In a recent paper Landman *et al.*[18] have carried out epitaxial growth of silicon using the Stillinger-Weber potential under conditions where the temperature of the

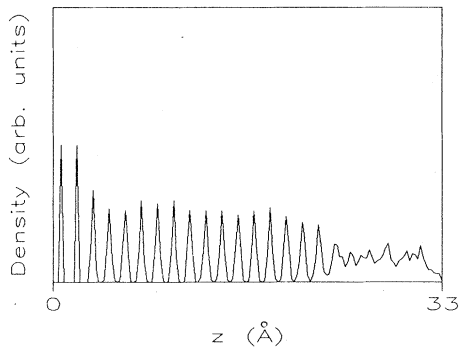

FIG 2. Density profile, in arbitrary units, at time step 50×10^3 into the 1450 K solidification simulation. Note the further growth of (001) planes as compared to Fig. 1.

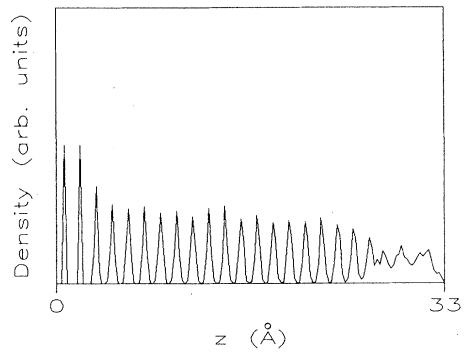

FIG. 3. Density profile, in arbitrary units, at time step 80×10^3 into the 1450 K solidification simulation. Note the additional (001) planes that have been formed after Fig. 2.

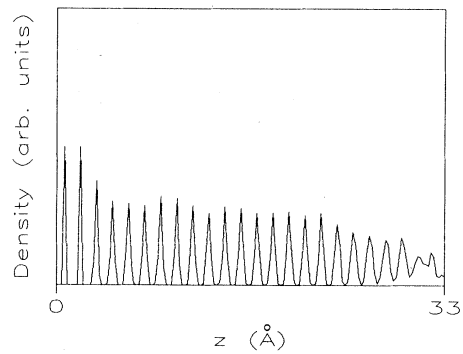

FIG. 4. Density profile, in arbitrary units, at time step 110×10^3 into the 1450 K solidification simulation showing the additional growth of (001) planes.

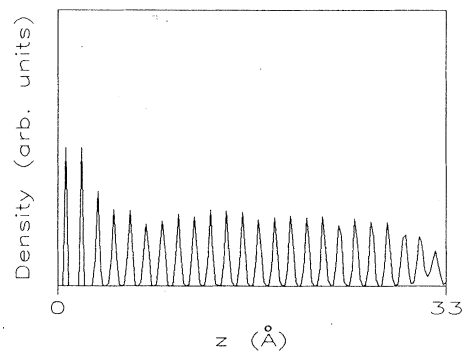

FIG. 5. Density profile, in arbitrary units, at time step 140×10^3 into the 1450 K solidification simulation. The growth of the system is complete at this time; further running of the system does not give a quantitative change in the density profile. The change in the density profile near the end of the sample, the last two planes before 33 Å, is associated with the free surface reconstruction.

system was not held constant. The authors of that paper were mainly interested in studying the microscopic growth processes. In contrast our main purpose is to determine the steady-state velocity versus temperature relation during solidification and melting.

In Figs. 6 and 7 we show the temperature profile of the system at 20×10^3 and 140×10^3 time steps into the simulation in arbitrary units. The temperature is defined as the average kinetic energy per particle. The temperature of the system is within a few degrees of the desired temperature, 1450 K for the present simulation, and there is not a noticeable temperature gradient in the bulk of the sample where the growth is taking place, which implies that the growth is approximately isothermal; of course, there must be a temperature gradient to conduct the latent heat of the transformation away from the interface to planes 3 and 4 where it is removed. The temperature profile of the system in all other growth and melting simulations has an appearance similar to Figs. 6 and 7.

Another way to monitor the growth of crystalline planes is through a coordination number profile. In Figs. 8 and 9 we show the coordination number profiles at 20×10^3 and 140×10^3 time steps into the simulation. The coordination number of the crystal is 4.0, while that of the supercooled liquid is higher, ≈4.6, due to the partial collapse of the tetrahedral structure in the liquid. In our previous study of the formation of amorphous silicon by rapidly cooling the liquid we found that the supercooled liquid has a coordination number of around 4.6[16,17] These coordination number profiles again show clearly the growth of the crystal with time.

We also monitored the two- and three-body potential energies, during the simulations. The three-body energy has a low value in the crystal due to the tetrahedral coordination of the particles and a higher value in the liquid. In Figs. 10 and 11 we show the three-body energy profiles in arbitrary units at 20×10^3 and 140×10^3 time steps into the growth. The growth of the crystal is again clearly shown in these figures. The two-body energy profiles

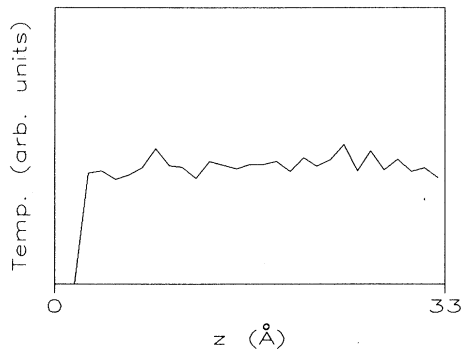

FIG. 6. Temperature profile, in arbitrary units, at time step 20×10^3 into the 1450 K growth simulation. This profile shows that the temperature remains approximately uniform along the sample during the growth. Energy is extracted at planes 3 and 4 on the left end of the system to keep the temperature of the system within a few degrees of the desired temperature. The temperature profile shows that there are not large temperature gradients in the system during the solidification.

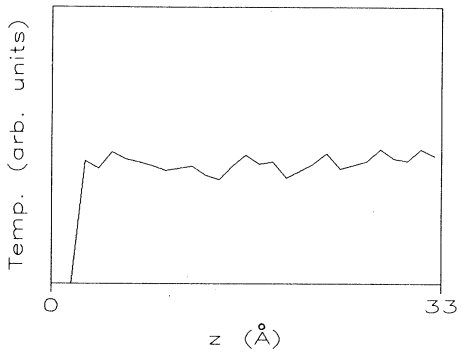

FIG. 7. Temperature profile, in arbitrary units at 140×10^3 time steps into the 1450 K solidification simulation which again shows that the temperature profile is approximately uniform over the sample.

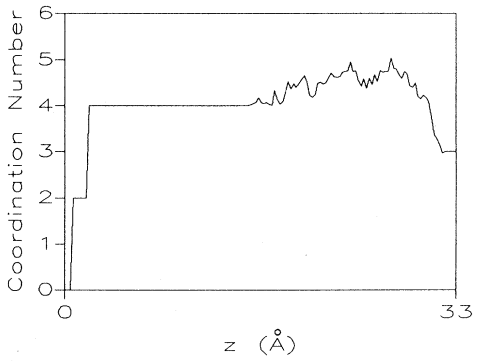

FIG. 8. Coordination number profile at time step 20×10^3 into the 1450 K solidification simulation showing the crystalline solid with coordination number 4.0 in contact with the supercooled liquid with coordination number ≈4.6. The coordination number of 2.0 on the left-hand side is for the first plane which has neighbors only on one side.

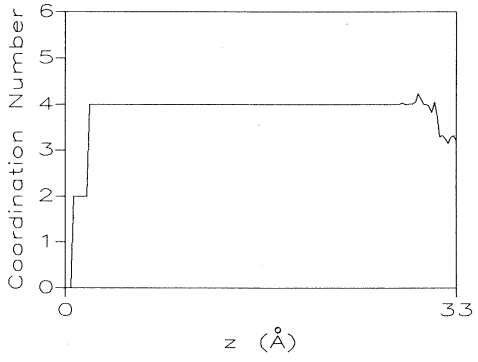

FIG. 9. Coordination number profile at time step 140×10^3 into the 1450 K solidification simulation. Comparison with Fig. 8 shows the further growth of the crystal that has occurred.

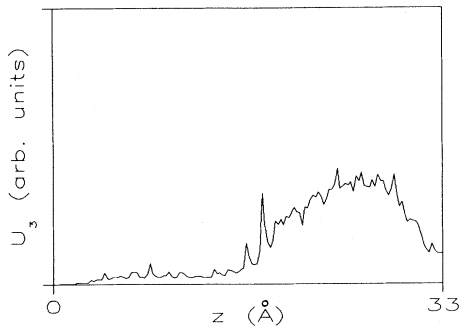

FIG. 10. Three-body energy profile, in arbitrary units, at time step 20×10^3 in the 1450 K solidification simulation. The three-body energy is smaller in the crystal due to the tetrahedral coordination.

show a decrease similar to the three-body increase during the growth process.

Note that the growth is completed at time step 140×10^3 in Fig. 5; running the simulation longer does not lead to a significant change in this figure or in other measures of the growth process. Figure 5 clearly shows that there is a (001) surface reconstruction at the free end of the sample. The nature of the (001) surface reconstruction for Stillinger-Weber silicon has been discussed by Abraham and Batra,[19] and Gawlinski and Gunton.[20] We have not yet studied the surface reconstruction in our samples, which are grown from the liquid, in detail.

IV. STEADY-STATE VELOCITY DETERMINATION

A. Solidification velocities

In order to determine the velocity of steady-state growth of the crystal we studied the time dependence of the arrival of the particles into the vicinity of their final positions in the crystal as a function of time. This was done by recording the final positions of the particles in their crystal-lattice positions at the end of the 150×10^3 time steps and then finding when the particles arrived in the vicinity of these positions. A particle was counted as being at its final lattice position if it were within half a nearest-neighbor distance of its final position in the crystal. The time dependence of the number of particles found in the vicinity of their final positions in the growing crystal gives the rate at which the crystal is growing as a function of time. A study of this number versus time shows that it has a linear portion as the growth proceeds. Performing linear regression on the linear portion of the number growth curve gives the steady-state velocity of solidification at the given temperature along with an error estimate. For the simulation at 1450 K we obtained a velocity of $v(T)=14.32\pm0.70$ m/s, which corresponds, on the average, to one plane growing every 9.67 ps.

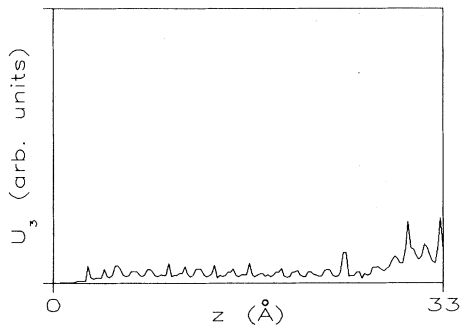

FIG. 11. Three-body energy profile, in arbitrary units, at time step 140×10^3 into the 1450 K solidification simulation. Note the further growth of the solid as shown by the smaller values of the three-body energy.

It is clear from studying figures such as Figs. 1–11 that several planes are growing at the same time so that one must be careful and not use times near the completion of the growth to determine the steady-state velocity for solidification. The same remarks are also valid in the case of melting. The fact that several planes are simultaneously forming or disorganizing during the growing and melting process has been noticed by earlier workers studying (001) Stillinger-Weber silicon. Note also that when we speak of the steady-state "velocity of the interface" or "growth velocity" in our computer experiments we mean the velocity determined from the linear portion of the number growth curve as explained above; the idea of a definite interface does not seem to be a useful quantitative concept in analyzing these computer growth experiments since several planes are growing at the same time. The most useful quantitative measure of growth that we have considered is the linear portion of the number growth curve which we have used to determine the steady-state velocities although there are other ways to quantify the growth and melting processes.

By carrying out similar 150×10^3 time step growth runs at 1050, 1250, 1350, and 1550 K we determined the steady-state growth velocities at these temperatures. At 1000 K the system shows growth of a few incomplete planes which we shall discuss in more detail later. At 950 K no growth of the system was observed over the 150×10^3 time steps. At the higher temperature end we observed no growth at 1600 and 1700 K over 150×10^3 time steps. The solidification velocities for all temperatures studied are shown in Table I along with results for melting which we discuss next.

B. Melting velocities

In order to determine the steady-state melting velocities we started with a crystallized sample, such as in Fig. 5, raised the temperature to a specified value and then ran the simulation in the same manner as explained above. We then determined the number of particles leaving the vicinity of their positions in the crystalline planes as a function of time. This number-versus-time relation has a linear portion consistent with our results for solidification. Using linear regression on this portion of the number growth relation leads to the steady-state velocity of melting along with an error estimate. We determined the velocities of melting at 1750, 1850, 1950, and 2050 K which are shown in Table I. As mentioned previously, at 1600 and 1700 K we did not observe any significant changes in the sample over the 150×10^3 time steps of the simulation.

TABLE I. Steady-state solidification (positive) and melting (negative) velocities as determined at each temperature using molecular-dynamics simulations. These are all the results obtained in the present study.

Temperature (K)	Velocity (m/s)	Process
950		no growth
1000	partial growth of a few planes	
1050	10.23±1.48	crystallization
1250	16.43±1.04	crystallization
1350	19.40±2.01	crystallization
1450	14.32±0.70	crystallization
1550	11.95±0.69	crystallization
1600		no growth
1700		no growth
1750	−21.22±1.04	melting
1850	−22.20±0.80	melting
1950	−43.00±1.92	melting
2050	−54.86±2.14	melting

V. RESULTS AND COMPARISON WITH THEORETICAL AND EXPERIMENTAL STUDIES

A. Results

In Table I and Fig. 12 we show all the steady-state velocity-versus-temperature values determined in this study; the simulation results are shown by the squares in Fig. 12. The maximum velocity of crystal growth that we found was $v(T)=19.40\pm2.01$ m/s at a temperature of 1350 K while at 950 K no growth was observed.

B. Comparison with theoretical studies

Most theoretical discussions in Refs. 1–9 are centered around the transition-state theory of crystal growth. For a discussion of transition-state theory see Jackson and Chalmers[10] and Jackson.[11] In this theory the rate of crystallization R_c is assumed to be controlled by the diffusion process in the liquid

$$R_c=C_1\exp[-Q/(k_BT)],\quad C_1=\text{const}\ , \tag{5.1}$$

where Q is the activation energy for viscous or diffusive motion in the liquid. For melting the rate R_m is assumed to be of the form

$$R_m=C_2\exp[-(Q+L)/(k_BT)],\quad C_2=\text{const}\ , \tag{5.2}$$

where $L=\Delta H$ is the heat of fusion of the phase transformation. Thus in the melting process the atoms must overcome the activation energy barrier $Q+L$. If T_0 is the equilibrium melting temperature then $R_c(T_0)=R_m(T_0)$, and we find

$$C_1/C_2=\exp(L/k_BT_0)\ . \tag{5.3}$$

The velocity of crystallization ($v>0$) or melting ($v<0$) is given by the difference between R_c and R_m

$$\begin{aligned}v(T)&=R_c-R_m\\&=C_1\exp(-Q/k_BT)\\&\quad-C_2\exp[-(Q+L)/k_BT]\ .\end{aligned} \tag{5.4}$$

Using Eqs. (5.1)–(5.3) this latter equation can be written

$$v(T)=C_3\exp(-Q/k_BT)[1-\exp(-L\,\Delta T/k_BT)]\ , \tag{5.5}$$

where $\Delta T=T_0-T$ and $C_3=C_1\exp(-L/k_BT_0)$ is another constant. This is the main equation of the transition-state theory in a convenient form for our purposes.

In order for Eq. (5.5) to give values for $v(T)$ we must know values for the four constants T_0, L, C_3, and Q. For T_0 we choose 1650 K which is consistent with no observed growth at 1600 and 1700 K in the simulations. In an earlier study of the melting of silicon we[21] determined $L=932$ J/g for Stillinger-Weber silicon; notice that this

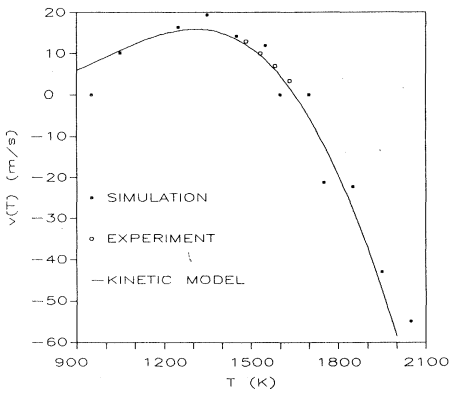

FIG. 12. The velocity-versus-temperature relation as determined in this study. The squares denote the points determined by our solidification and melting simulations and are the values shown in Table I. The solid curve is the transition-state theory prediction, Eq. (5.5) for $T_0=1650$ K, $L=932$ J/g, $Q=0.42$ eV, and $C_3=1700$ m/s. The four open circles are experimental values obtained from the results of Ref. 4 for the (001) epitaxial solidification of crystalline silicon.

is approximately half the observed value of L. From the Arrhenius plot of the diffusion constant in the paper of Broughton and Li[22] we may determine the activation energy for diffusion to be $Q=0.42$ eV. The constant C_3 is not yet determined since there is no way to determine an accurate value of C_1. We choose $C_3=1700$ m/s which then allows the relation $v(T)$ to be given in Fig. 12 as the full line. The only adjustable parameter in Eq. (5.5) is C_3 which has been chosen so as to get a good fit to the simulation values. Alternatively we could choose C_3 so that the velocity at one particular temperature was given by Eq. (5.5).

The general agreement between the transition-state theory, Eq. (5.5), and the simulation values shown in Fig. 12 is good qualitatively, but there are serious quantitative discrepancies including the value v(950 K) where Eq. (5.5) gives 7.5 m/s, whereas the simulation gave zero for this velocity. Of course, it would be overly optimistic to expect this simple theory to describe in quantitative detail such complicated, nonequilibrium, many-body processes. In summary one can state that the transition-state theory gives a reasonable qualitative description of the heterogeneous crystallization and melting of Stillinger-Weber silicon.

C. Experimental results

As a note of caution we remark that the simulations that we are reporting are calculations on a particular model of silicon.[13] The Stillinger-Weber potential is a simple model potential, and certainly we cannot expect agreement with all of the very complicated results discussed in the literature.[1–9] One of the main disagreements between our simulations and experimental results is that above an epitaxial [001] growth velocity of ≈ 15 m/s (undercooling of ≈ 250 K) silicon is observed to solidify into the amorphous phase instead of the crystalline phase.[2] We do not see this behavior in our simulations, the velocity of growth into the crystalline phase increases to a maximum value at 1350 K and then decreases to at least 1050 K.

In Fig. 12 we have also shown the experimental velocity-versus-temperature relation for solidification for velocities below the critical velocity for [001] amorphization, as reported by Galvin *et al.*[4] These points are marked with open circles in Fig. 12 and are for temperatures of 1483, 1533, 1583, and 1633 K; what is presented in Ref. 4 is a continuous curve of values of v and T and what we have shown is four points from this continuous curve. There is excellent agreement between these experimental values, the results from our simulations, and the transition-state theory, Eq. (5.5). Using velocities less than 6 m/s, Galvin *et al.* report a temperature-versus-velocity slope of $(-15\pm 5$ K)/(m/s) while the slope of Eq. (5.5) at the melting point is -9.8 K/(m/s).

Unfortunately we cannot compare our simulation results for solidification, at undercooling temperatures below 250 K with the experimental results since, as mentioned above, experimentally the system grows into amorphous silicon whereas we find that the Stillinger-Weber system continues to grow into crystalline silicon down to a temperature of at least 1050 K. This is consistent with the fact, mentioned earlier, that Stillinger-Weber amorphous silicon is not easily formed by cooling the liquid.

For melting we have the experimental result that for a velocity of melting of -190 m/s the temperature must be less than 3300 K.[5] If we use Eq. (5.5) we find $v=-190$ m/s for $T=2424$ K. Thus, the extrapolation of our results using the transition-state equation is consistent with this experimental bound. We plan to perform more melting simulations at higher temperatures. Near the boiling point 3500 K, Eq. (5.5) gives a melting velocity of -617 m/s.

D. Growth at 1000 K

At 1000 K the system partially grew a few incomplete planes of particles whose average coordination numbers were close to those for our models of amorphous silicon, namely 4.1–4.3. In Fig. 13 we show the density profile for the 1000 K simulation, in arbitrary units, at the end of the simulation. In this case the simulation was extended to 210×10^3 time steps to see if any further growth would occur; as can be seen from Fig. 13 the system did not grow to completion even with this longer simulation. From Fig. 13 it is clear that some incomplete planes have grown, planes 16–18, which have spacing along the [001] direction close to the spacing for the crystalline planes, but for which particles are missing and out of place as indicated by the density profile not extending to zero. The coordination number profile in Fig. 14 shows that the portion of the sample containing these planes has an average coordination number around 4.2 which, as we have mentioned before, is the approximate value for Stillinger-Weber amorphous silicon. The three-body energy profile in Fig. 15 also indicates that this portion of the sample is not crystalline by the higher value of the three-body energy. Note, however, that this three-body energy is not as large as for the supercooled liquid phase as can be seen by comparison to Fig. 10. These results

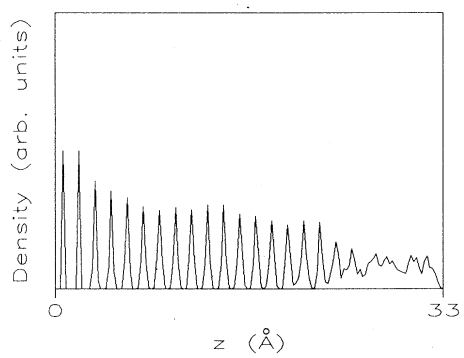

FIG. 13. The density profile, in arbitrary units, at time step 210×10^3 for the 1000 K solidification simulation. This shows that planes 16, 17, and 18 have partially grown at this temperature. The noncrystallinity of this portion of the sample can be seen by the density profile not going to zero between the planes which implies that particles are not only in crystalline positions. We suggest that this represents the growth into amorphous silicon, although more studies must be carried out to resolve this point.

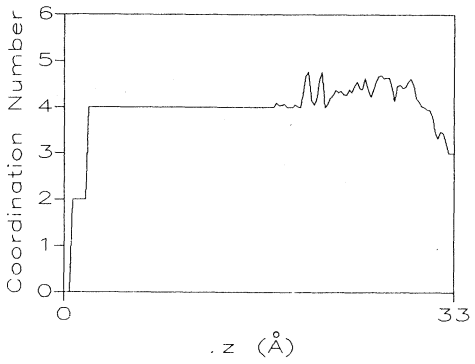

FIG. 14. The coordination number profile at time step 210×10^3 into the 1000 K solidification simulation. The planes 16, 17, and 18 have an average coordination number of ≈ 4.2 which is the approximate coordination number of Stillinger-Weber amorphous silicon.

lead us to suggest that at 1000 K the system has partially grown into amorphous Stillinger-Weber silicon. We plan to study the growth further at these lower temperatures to determine whether Figs. 13–15 are associated with the growth of amorphous silicon.

VI. SUMMARY AND CONCLUSIONS

The steady-state velocity-versus-temperature relation for [001] liquid epitaxial growth of Stillinger-Weber silicon has been determined by carrying out approximately isothermal solidification and melting simulations. At each temperature the growth or melting simulation is of duration 115 ps, this time was selected by growing the 1450 K simulation to completion. The temperature of the system is held constant by removing energy equal to the latent heat of transformation at planes far removed from the growth region. The results for all simulations are given in Table I and Fig. 12.

The growth velocity for undercooling temperatures down to 250 K agrees well with published results in Ref. 4. The simulation data is fit qualitatively by the transition-state formula, Eq. (5.5) parametrized to Stillinger-Weber silicon. The temperature versus slope at the melting point is -9.8 K/(m/s) for the simulation compared to $(-15\pm5$ K)/(m/s) in Ref. 4. Note that the transition-state theory Eq. (5.5) also gives a good fit to the experimental results of Galvin *et al.*, even though we have used the parameters of Stillinger-Weber silicon. For example, we used the latent heat of fusion $L=932$ J/g, where experimentally the heat of fusion is 1800 J/g.

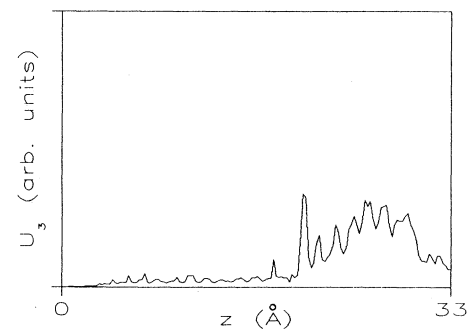

FIG. 15. The three-body energy profile, in arbitrary units, at time step 210×10^3 into the 1000 K solidification simulation. The three-body energy is larger for the noncrystalline region of the sample mentioned in Figs. 13 and 14 which supports our conjecture that this represents growth into an amorphous like structure.

The simulation velocity-versus-temperature relation gives good agreement with the experimental literature above 1350 K, however, the simulation gives growth into a crystal for undercooling below the critical value for amorphization. The reason for this is that Stillinger-Weber amorphous silicon does not form easily upon rapidly cooling the liquid. At the high-temperature end we find $v=-190$ m/s at 2424 K from Eq. (5.5), whereas the experimental limit is $T<3300$ K for this velocity.

In the 1000 K growth simulation we observed the growth of a few incomplete planes which may be associated with the growth of the system into an amorphous-like structure. The velocity-versus-temperature relation determined by simulation shows a clear asymmetry about the melting point T_0, $|v(T_0-T)|=|v(T-T_0)|$ but shows no discontinuity in slope when passing through the melting point.

Our results for liquid epitaxial growth of silicon are important for studies attempting to model the growth of layered structures by atom deposition using molecular dynamics and the Stillinger-Weber potential.[20,23] These atom deposition simulations are attempts to model molecular beam epitaxial growth. As recently shown[24] in single-atom deposition the deposited atoms in such simulations of silicon have large kinetic energies and are very slow to reach thermal equilibrium with the substrate. Our results show that large liquid-epitaxial-growth velocities of 10 m/s [13.6 ps per (001) plane] occur for temperatures as low as 1050 K or 60% of the melting temperature with the Stillinger-Weber potential. This lends support to the suggestion in Ref. 24 that in earlier deposition growth studies using the Stillinger-Weber potential the crystal growth may have been more like liquid epitaxial growth.

One question in studies such as presented in this paper is how the results are changed if a different number of particles were used in the simulation. We carried out [001] growth simulations with 1152 particles. In this simulation there are 36 (001) planes with each plane having 32 particles. The growth of the planes occurs in the same general way in this larger system. We also carried out simulations with a system of 1530 particles in which the growth of the planes was similar. For these larger particle numbers we did not carry out detailed simulations to obtain accurate growth velocities so the question of the number dependence of the growth and melting velocities in Table I cannot be estimated without further simulations. Gilmer[25] and colleagues have carried out growth and melting simulations for Stillinger-Weber silicon for larger systems and found results in general agreement with our results. They have also prepared interesting movies of the growth process which show the microscopic growth and melting processes.

ACKNOWLEDGMENTS

One of us (J.R.R.) thanks Dr. J. Y. Tsao, Dr. D. H. Lowndes, and Dr. P. Richards for helpful discussions. The calculations reported on in this paper were carried out on the Clemson University Computer System. We thank Dr. C. J. Duckenfield, Vice Provost of the Division of Computing and Information Technology, for allowing us to use these resources.

---

*Present address: Materials Science Division, Argonne National Laboratory, Argonne, IL 60439-4843.

[1]G. J. Galvin, M. O. Thompson, J. W. Mayer, P. S. Peercy, R. B. Hammond, and N. Paulter, Phys. Rev. B **27**, 1079 (1983).

[2]M. O. Thompson, J. W. Mayer, A. G. Cullis, H. C. Webber, N. G. Chew, J. M. Poate, and J. C. Jacobson, Phys. Rev. Lett. **50**, 896 (1983).

[3]M. O. Thompson, G. J. Galvin, J. W. Mayer, P. S. Peercy, J. M. Poate, D. C. Jacobson, A. G. Cullis, and N. G. Chew, Phys. Rev. Lett. **52**, 2360 (1984).

[4]G. J. Galvin, J. W. Mayer, and P. S. Peercy, Appl. Phys. Lett. **46**, 644 (1985).

[5]J. Y. Tsao, M. J. Aziz, M. O. Thompson, P. S. Peercy, Phys. Rev. Lett. **56**, 2712 (1986).

[6]B. C. Larsen, J. Z. Tischler, and D. M. Mills, J. Mater. Res. **1**, 144 (1986).

[7]J. Y. Tsao and P. S. Peercy, Phys. Rev. Lett. **58**, 2782 (1987).

[8]J. Y. Tsao, P. S. Peercy, and M. O. Thompson, J. Mater. Res. **2**, 91 (1987).

[9]D. H. Lowndes, S. J. Pennycook, R. F. Wood, G. E. Jellison, Jr., and S. P. Withrow, in *Materials Research Society Symposium Proceedings* (MRS, Pittsburgh, 1988), Vol. 100, p. 489.

[10]K. A. Jackson and B. Chalmers, Can. J. Phys. **34**, 473 (1956).

[11]K. A. Jackson, in *Crystal Growth and Characterization,* edited by R. Ueda and J. B. Mullin (North-Holland, Amsterdam, 1985).

[12]M. D. Kluge and J. R. Ray, Bull. Am. Phys. Soc. **33**, 1371 (1988).

[13]F. H. Stillinger and T. A. Weber, Phys. Rev. B **31**, 5162 (1985).

[14]M. D. Kluge and J. R. Ray, Phys. Rev. B **37**, 4132 (1988).

[15]J. Q. Broughton and F. F. Abraham, J. Cryst. Growth **75**, 613 (1986).

[16]M. D. Kluge and J. R. Ray, Bull. Am. Phys. Soc. **32**, 456 (1987).

[17]M. D. Kluge, J. R. Ray, and A. Rahman, Phys. Rev. B **36**, 4234 (1987).

[18]U. Landman, W. D. Luedtke, M. W. Ribarsky, R. N. Barnett, and C. L. Cleveland, Phys. Rev. B **37**, 4637 (1988).

[19]F. F. Abraham and I. P. Batra, Surf. Sci. **163**, L572 (1985).

[20]E. T. Gawlinski and J. D. Gunton, Phys. Rev. B **36**, 4774 (1987).

[21]M. D. Kluge, J. R. Ray, and A. Rahman, J. Chem. Phys. **85**, 4028 (1986).

[22]J. Q. Broughton and X. P. Li, Phys. Rev. B **35**, 9120 (1987).

[23]M. Schneider, I. K. Schuller, and A. Rahman, Phys. Rev. **36**, 1340 (1987).

[24]R. Biswas, G. S. Grest, and C. M. Soukoulis Phys. Rev. B **38**, 8154 (1988).

[25]G. H. Gilmer (private communication).